

# Stokes and anti-Stokes Raman spectra of the high energy C-C stretching modes in graphene and diamond

Ado Jorio<sup>\*1</sup>, Mark Kasperczyk<sup>2</sup>, Nick Clark<sup>and</sup><sup>3</sup>, Elke Neu<sup>4,5</sup>, Patrick Maletinsky<sup>4</sup>, Aravind Vijayaraghavan<sup>3</sup> and Lukas Novotny<sup>2</sup>

<sup>1</sup> Departamento de Física, Universidade Federal de Minas Gerais, Belo Horizonte, MG 31270-901, Brazil

<sup>2</sup> Photonics Laboratory, ETH Zürich, 8093 Zürich, Switzerland

<sup>3</sup> School of Materials and National Graphene Institute, University of Manchester, Manchester M13 9PL United Kingdom

<sup>4</sup> Department of Physics, University of Basel, Klingelbergstrasse 82, CH-4056 Basel, Switzerland. <sup>5</sup> Present address: Universität des Saarlandes, Experimentalphysik Building E2.6, Office 2.19 D-66123, Saarbrücken, Germany.

**Keywords** Graphene, Diamond, Raman spectroscopy, anti-Stokes scattering.

\* Corresponding author: e-mail [adojorio@fisica.ufmg.br](mailto:adojorio@fisica.ufmg.br), Phone: +55 31 34096610, Fax: +55 31 34095600

The Stokes and the anti-Stokes Raman spectra from the high energy carbon-carbon stretching modes in graphene and diamond are studied, with focus on their intensity dependence on the excitation laser power. For diamond, the experiment was performed on a 50 $\mu$ m slice of chemical vapour deposition grown single crystal, using a 785nm laser, both in the continuous wave (CW) and pulsed mode locked (ML – 130fs pulses) excitation regimes. For graphene, the experiments were performed on suspended samples, including single layer, bilayer with AB-Staking, twisted bi-layer, and a sample with 4-6 layers, using a  $\lambda$ =532nm and a  $\lambda$ =633nm laser. The Stokes and anti-Stokes intensities vary largely from sample to sample, and the anti-Stokes/Stokes intensity ratio shows different excitation laser power behaviours. These differences can be explained on the basis of laser heating or correlated Stokes-anti-Stokes scattering phenomena.

**1 Introduction** Phonons are quantum states of the harmonic oscillators, having their increase and decrease in number  $n$  described by creation ( $a^\dagger$ ) and annihilation ( $a$ ) operators. The action of these operators on an eigenstate  $|n\rangle$  introduces normalization factors given by  $a^\dagger|n\rangle = (n+1)^{1/2}|n+1\rangle$  and  $a|n\rangle = n^{1/2}|n-1\rangle$ . In the inelastic scattering of light by phonons, a photon creates or annihilates a phonon, in the so-called Stokes or anti-Stokes Raman scattering process. The intensity ratio between the Stokes and anti-Stokes components ( $I_{as}/I_s$ ) are, therefore, usually determined by the quantum mechanics normalization factors,  $I_{as}/I_s = n/(n+1)$  [1,2].

The thermal population of phonons is given by the Bose-Einstein distribution function  $n_0 = [\exp(E_q/k_B T) - 1]^{-1}$ , where  $E_q$  and  $k_B T$  are the phonon and thermal energies, respectively. Replacing  $n$  by  $n_0$  in the anti-Stokes/Stokes intensity ratio gives  $I_{as}/I_s = (n_0+1)/n_0 = C \exp(E_q/k_B T)$ . This equation can be inverted to obtain the effective phonon temperature in a material by measuring their Stokes and anti-Stokes Raman spectra, given by  $T = E_q / \{k_B [\ln C - \ln(I_{as}/I_s)]\}$ . This procedure has been largely used in the literature to study the phonon population dependence of dif-

ferent nanomaterials properties, including electrical power [3], thermal conductivity [4], effective temperatures on biased nanostructures [5], phonon anarmonicities and lifetimes [6,7], and optical transitions [8,9]. Generally, the constant  $C$  is found by setting  $T$  at room temperature for very low laser power (or zero bias), where sample heating should not be present.

One aspect that is not considered in this type of treatment is the possibility that one single phonon that is created in the Stokes process is subsequently annihilated in the anti-Stokes process. This correlated Stokes-anti-Stokes scattering phenomenon was proposed in 1977 by Klyshko [10], and it has been shown to affect the anti-Stokes and Stokes intensities in graphene [11] and diamond [12,13]. A theoretical framework to address this phenomenon has been proposed, demonstrating implications for the anti-Stokes/Stokes intensity ratio [14].

In this paper we will explore the laser power dependence for diamond and graphene, including the dependence on the layer stacking, on different excitation laser energies, and on the difference between a continuous wave (CW) or a mode locked pulsed (ML) laser regime. Some of the re-

sults shown here have already been discussed in Refs.[11,13,14], and here we present a deeper comparative analysis. The differences can be explained on the basis of laser heating or correlated Stokes-anti-Stokes scattering (SaS) phenomena.

## 2 Methods

**2.1 Samples** Graphene and diamond samples are studied here. Graphene has a first-order Raman allowed peak at  $1584\text{cm}^{-1}$ , named G band. Diamond has a first-order Raman allowed peak at  $1332\text{cm}^{-1}$ . In both cases, these Raman bands are related on the C-C stretching modes.

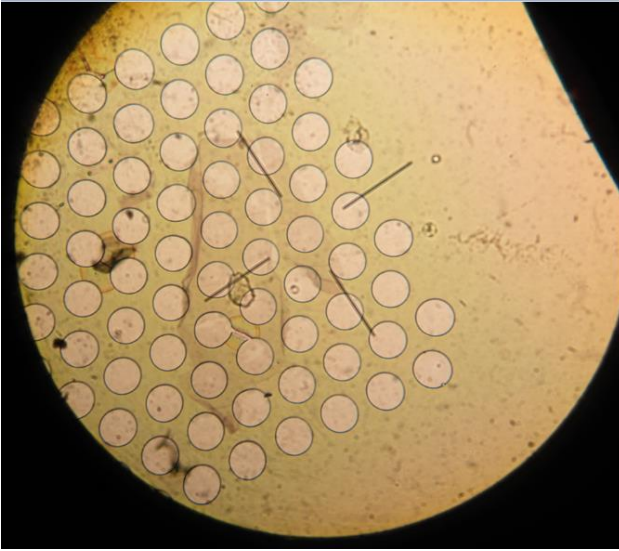


**Figure 1** Optical image of the graphene sample. The holes in the  $\text{SiN}_x$  substrate are  $10\mu\text{m}$  in diameter.

The diamond sample was grown by the chemical vapour deposition (CVD) method, with cutting and polishing generating a highly pure free-standing  $50\mu\text{m}$  thick diamond crystal [13]. As for the graphene samples, Fig.1 shows an optical image. The graphene sample has been deposited on top of a  $\text{SiN}_x$  substrate with holes. The graphene flakes are suspended over the holes, and the light can pass through the graphene sample without touching the substrate. More details can be found in Ref.[11]. Four types of graphene samples are studied here: single-layer graphene, double-layer graphene with AB-stacking, twisted bilayer graphene (tBLG), and a 4-6 layers graphene with AB-stacking. All the samples were prepared by mechanical exfoliation of graphite, and deposited on a similar substrate, as shown in Fig.1(a). The tBLG [15] was engineered to exhibit a twist angle  $\theta = 11^\circ$ , which generates a peak in the joint density of states that lies in the energy range of a  $633\text{nm}$  and a  $532\text{nm}$  lasers [11]. In this way, when exciting the tBLG with a  $633\text{nm}$  laser, the G band

anti-Stokes Raman emission is resonant. When exciting the tBLG sample with the  $532\text{nm}$  laser, the G band Stokes Raman emission is resonant.

**2.2 Experimental details** The graphene samples were excited with a frequency doubled Nd:YVO<sub>4</sub> laser at  $E_{\text{laser}} = 2.33\text{ eV}$  ( $\lambda_{\text{laser}} = 532.0\text{ nm}$ ) and with a HeNe laser at  $E_{\text{laser}} = 1.96\text{ eV}$  ( $\lambda_{\text{laser}} = 632.8\text{ nm}$ ), both working in the continuous wave (CW) regime. As already specified, these two lasers are off resonance with respect to the peak in the joint density of states (JDOS) for the tBLG,  $E_{\text{laser}}$  being blue- or red-shifted from the JDOS peak by approximately the G band phonon energy ( $E_G = 0.2\text{ eV}$ ) [11]. The signal was collected through a spectrometer, equipped with a charge coupled device (CCD) detector, and filtered using optical notches and band pass filters.

The diamond sample was studied with a Ti:Sapph laser at  $\lambda = 785\text{nm}$ , which can work both in the CW (continuous wave) and ML (mode locked – pulsed) regimes. For ML, the duration of the excitation laser pulses is  $\tau = 130\text{fs}$ , with a repetition rate of  $\Delta f = 76\text{MHz}$ .

Finally, a  $130\text{fs}$  pulsed laser at  $\lambda = 545\text{nm}$  from an OPO was used to excite both diamond and one of the graphene samples, for comparative analysis.

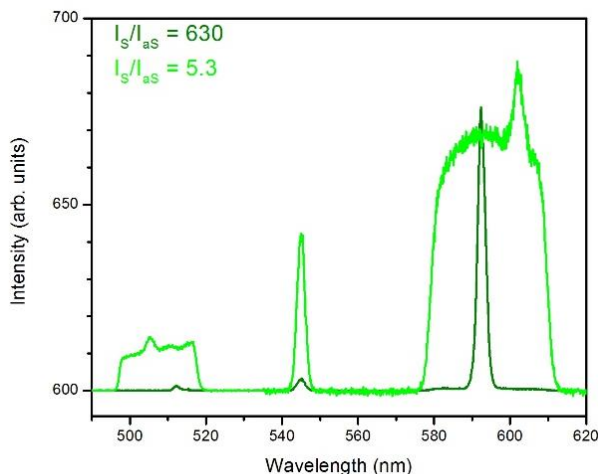
## 3 Results and discussions

**3.1 Pulsed laser Raman spectra** Figure 2 shows the Stokes and anti-Stokes Raman spectra of the 4-6 layers graphene and diamond samples, obtained with a  $130\text{fs}$  pulsed laser at  $\lambda = 545\text{nm}$ , with average excitation laser power  $P_{\text{laser}} = 20\text{mW}$ . For diamond (olive lines), the central peak at  $\lambda = 545\text{nm}$  is leakage from the laser, and the peaks at  $512\text{nm}$  and  $592\text{nm}$  are the anti-Stokes and Stokes Raman peaks, respectively. The width of the peaks is determined by the spectral width of the  $130\text{fs}$  laser pulses.

For graphene (light green in Fig.2), again the peak at  $\lambda = 545\text{nm}$  is leakage from the laser, while the anti-Stokes and Stokes Raman peaks appear at wavelengths ( $505\text{nm}$  and  $602\text{nm}$ , respectively), which are different from those in diamond, since the phonon energy is different. To measure the Raman signals, we used a band-pass filter at  $(506 \pm 20)\text{nm}$  for the anti-Stokes signal, and a band-pass filter at  $(600 \pm 20)\text{nm}$  for the Stokes signal. The square-shaped signals observed within these ranges in Fig.2 come from the hot luminescence of graphene, which appears when graphene is excited with pulsed lasers [16].

Analysing the Raman peak intensities with a single Lorentzian fit, we found the Stokes/anti-Stokes intensity ratio for diamond  $I_S/I_{AS} = 630$ , which is close to the expected value for the diamond phonon ( $1332\text{cm}^{-1}$ ), in agreement with the Bose-Einstein phonon population at room temperature ( $T = 295\text{K}$ ). For the graphene sample (G band at  $1584\text{cm}^{-1}$ ), the Stokes/anti-Stokes intensity ratio is  $I_S/I_{AS} = 5.3$ , which is three orders of magnitude smaller

1 than the expected value from the Bose-Einstein phonon  
 2 population at room temperature. This result indicates that  
 3 either the graphene sample exhibits a very high laser-  
 4 induced phonon temperature, or that the Stokes-anti-Stokes  
 5 correlated scattering phenomenon is the dominating pro-  
 6 cess. Correlation measurements, as performed in  
 7 Refs.[12,13] are not possible here due to the strong hot lu-  
 8 minescence [16].



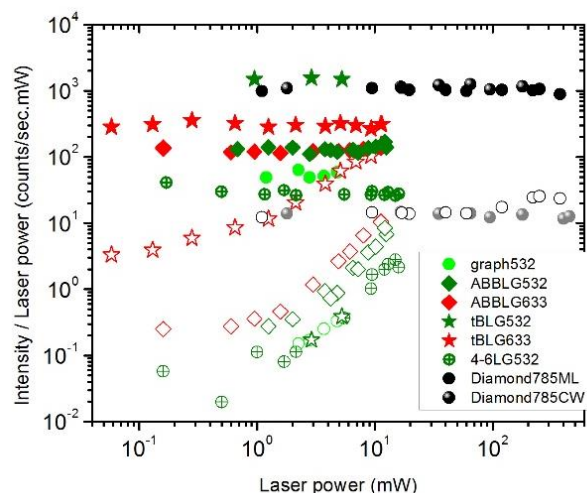
11 **Figure 2** Stokes and anti-Stokes Raman spectra of graphene  
 12 (light green) and diamond (olive) obtained with a 130fs pulsed laser  
 13 at  $\lambda=545\text{nm}$ . The Stokes/anti-Stokes intensity ratio ( $I_S/I_{aS}$ ) is  
 14 also displayed for both samples, following the same colour code.  
 15 The  $1332\text{cm}^{-1}$  diamond peak appear at  $592\text{nm}$  and  $512\text{nm}$  for the  
 16 Stokes and anti-Stokes scattering, respectively. The  $1584\text{cm}^{-1}$   
 17 graphene peak appears at  $602\text{nm}$  and  $505\text{nm}$  for the Stokes and  
 18 anti-Stokes scattering, respectively.

19 **3.2 Spectral power dependence** Figure 3 shows  
 20 the excitation laser power dependence for the Stokes and  
 21 anti-Stokes intensities normalized by the excitation laser  
 22 power, from all the samples studied in this work. Green,  
 23 red and black/grey symbols indicate Raman spectra obtained  
 24 with the lasers at  $\lambda_{\text{laser}} = 532.0\text{ nm}$ ,  $\lambda_{\text{laser}} = 632.8\text{ nm}$   
 25 and  $\lambda_{\text{laser}} = 785\text{ nm}$ , respectively. The different symbol  
 26 shapes indicate the specific samples, as displayed in the  
 27 figure legend. Graphene data were obtained with CW lasers.  
 28 Filled and opened symbols stand for Stokes and anti-  
 29 Stokes intensities, respectively, except for diamond with  
 30 the CW laser, where black and grey stand for Stokes and  
 31 anti-Stokes intensities, respectively.

32 In Fig.3, the laser-power normalized Stokes intensities  
 33 (filled symbols) show a constant value, in agreement with  
 34 a linear dependence of  $I_S$  on the excitation laser power.  
 35 The laser-power normalized anti-Stokes intensities exhibit  
 36 a super-linear power dependence. Therefore, the anti-  
 37 Stokes responses demonstrate that either laser-induced

heating or correlated Stokes-anti-Stokes scattering are tak-  
 ing place.

Figure 4 shows more clearly the behaviour of the dia-  
 mond Raman responses. For CW excitation, both Stokes  
 (black spheres) and anti-Stokes (grey spheres) exhibit a  
 linear dependence with the excitation laser power, which is  
 evident in Fig.4 by a constant value for “Intensity/Laser  
 power”. For the ML pulsed excitation, the Stokes spectra  
 (black circles) shows a linear dependence on the excitation  
 laser power, evidenced by a constant “Intensity/Laser  
 power” in Fig.4, while the anti-Stokes (open circles) shows  
 a super-linear dependence.



38 **Figure 3** Laser power dependence for the Stokes and anti-Stokes  
 39 scattering intensities for diamond and different graphene samples.  
 40 The different samples are indicated by different symbols, according  
 41 to the legend: graph532 – single layer graphene excited with  
 42  $\lambda=532\text{nm}$ ; ABBLG532 – AB-stacked bilayer graphene excited  
 43 with  $\lambda=532\text{nm}$ ; ABBLG633 – AB-stacked bilayer graphene excited  
 44 with  $\lambda=633\text{nm}$ ; tBLG532 – twisted bilayer graphene excited  
 45 with  $\lambda=532\text{nm}$ ; tBLG633 – twisted bilayer graphene excited  
 46 with  $\lambda=633\text{nm}$ ; 4-6LG532 – 4 to 6-layers graphene with AB-  
 47 stacking excited with  $\lambda=532\text{nm}$  (graphene data were obtained  
 48 with CW lasers); Diamond785ML – diamond excited with  
 49  $\lambda=785\text{nm}$  in the pulsed mode locked regime; Diamond785CW –  
 50 diamond excited with  $\lambda=785\text{nm}$  in the continuous wave regime.

51 **3.3 anti-Stokes/Stokes intensity ratio** Figure 5  
 52 shows the excitation power dependence behaviour for the  
 53  $I_{aS}/I_S$  intensity ratio for all the samples studied in this work.

54 For diamond,  $I_{aS}/I_S$  is constant for the CW excitation  
 55 (black circles). This indicates that neither heating nor the  
 56 correlated Stokes-anti-Stokes scattering phenomena are relevant  
 57 [17]. However, for the pulsed ML excitation, the behaviour is  
 super-linear. It has been shown already that this super-linear  
 behaviour is due to the correlated Stokes-anti-Stokes scattering  
 (SaS) process [12-14]. Since the SaS is a non-linear process,  
 the ultra-high intensities within a

pulse in the ML pulsed laser regime are needed to produce the effect in diamond.

For graphene, a difference in behaviour is observed when comparing the tBLG in resonance with the anti-Stokes photon emission (red star data) and all the other samples. The data are fit with the theory introduced in Ref.[14]. The fittings of the excitation laser power dependences for single layer graphene (light green circle), AB-stacked bilayer graphene (diamond symbols), and 4-6-layers graphene (crossed circles) indicate an  $I_{as}/I_s$  dependence dominated by thermal effects. The fitting of the excitation laser power dependence for twisted bilayer graphene in resonance with the anti-Stokes photon emission (red star data) indicates an  $I_{as}/I_s$  dependence dominated by the SaS correlated scattering, consistent with Ref.[14]. For tBLG in resonance with the Stokes photon emission (green star data), only two data points are obtained due to the very low anti-Stokes intensity, which is not enough data for a fitting analysis. For graphene all the spectra were obtained in the CW excitation regime.

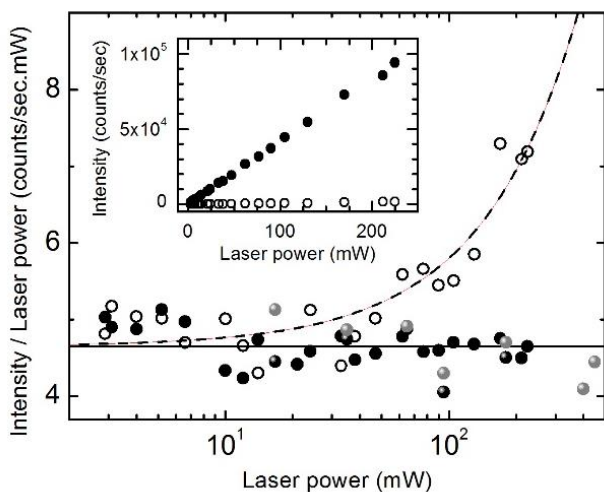


**Figure 4** Excitation laser power dependence for the Stokes and anti-Stokes Raman intensities for diamond, normalized (1) by the laser power and (2) by a constant factor to merge the Stokes and anti-Stokes intensities. Black and grey spheres stand for Stokes and anti-Stokes Raman intensities obtained in the CW excitation regime. Filled and open circles stand for the Stokes and anti-Stokes Raman intensities obtained in the pulsed ML excitation regime. For the spectra obtained in the ML pulsed regime, laser power means the average laser power, and not the peak laser power. The inset shows the Stokes and anti-Stokes intensities as measured in the pulsed ML regime, in a linear scale.

When comparing graphene and diamond, the first important difference is the phonon energy, which influences on the Bose-Einstein distribution. Additionally, diamond is transparent for visible and lower light energies, while graphene is always in resonance with the light absorption and emission. The SaS phenomenon appears here in diamond when ultra-high intensities from a pulsed laser is in place,

while the specially engineered tBLG shows the phenomenon at much lower average powers, even for a CW laser. More work is needed to characterize the SaS process in graphene, especially because the strong hot luminescence prevents the use of pulsed lasers for photon coincidence experiments.

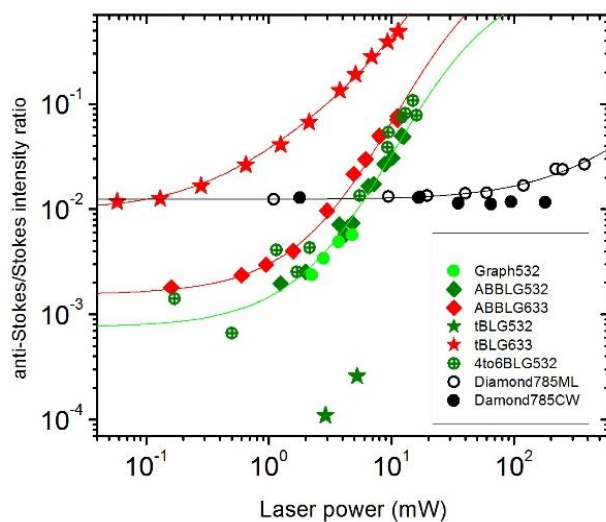


**Figure 5** Excitation laser power dependence for the anti-Stokes/Stokes Raman intensity ratio ( $I_{as}/I_s$ ) for diamond (black data) and for the different graphene samples (green and red data). Sample specification is found in the figure legend: graph532 – single layer graphene excited with  $\lambda=532\text{nm}$ ; ABBLG532 – AB-stacked bilayer graphene excited with  $\lambda=532\text{nm}$ ; ABBLG633 – AB-stacked bilayer graphene excited with  $\lambda=633\text{nm}$ ; tBLG532 – twisted bilayer graphene excited with  $\lambda=532\text{nm}$ ; tBLG633 – twisted bilayer graphene excited with  $\lambda=633\text{nm}$ ; 4-6BLG532 – 4 to 6-layers graphene with AB-stacking excited with  $\lambda=532\text{nm}$ ; Diamond785ML – diamond excited with  $\lambda=785\text{nm}$  in the pulsed mode locked regime; Diamond785CW – diamond excited with  $\lambda=785\text{nm}$  in the continuous wave regime. The lines are fitting to the data according with the theory presented in Ref.[14].

**3 Conclusions** In this work we measured the power dependence of the Stokes and anti-Stokes intensities from a  $50\mu\text{m}$  thick diamond crystal and from different graphene samples, including single layer, bilayer and 4 to 6-layers graphenes. The  $I_{as}/I_s$  intensity ratio varies from sample to sample, and it also depends on the excitation regime (pulsed vs. continuous wave). The results are analysed considering two distinct effects, namely laser induced heating and the production of correlated Stokes-anti-Stokes photon pairs.

Our results indicate that there is no heating in Diamond. For CW laser excitation, this is proven by a constant value of the  $I_{as}/I_s$  ratio. For the pulsed laser excitation, the increase in the  $I_{as}/I_s$  ratio comes from the correlated Stokes-anti-Stokes phenomenon. For graphene, the correlated Stokes-anti-Stokes phenomena is dominant for tBLG when

in resonance with the scattered anti-Stokes emission. Otherwise, heating is the dominant phenomenon.

**Acknowledgements** A.J. acknowledges CAPES and ETH for financing his visit to ETH Zurich, and CNPq grant 460045/2014-8. L.N. thanks financial support by the Swiss National Science Foundation (SNF) through Grant 200021-14 6358. A.V. thanks the Engineering and Physical Sciences Research Council (EPSRC) for financial support through Grants EP/G035954/1 and EP/K009451/1.

## References

- [1] Raman, C. V. and Krishnan, K. S. A new type of secondary radiation. *Nature (London)* 121, 501 (1928).
- [2] Jorio, A. Dresselhaus, M. S. Saito, R. *Raman Spectroscopy in Graphene Related Systems* (Wiley-VCH, 2011).
- [3] Steiner, M. et al. Phonon populations and electrical power dissipation in carbon nanotube transistors. *Nature Nanotech.* 4, 320 (2009).
- [4] Faugeras, C. et al. Thermal Conductivity of Graphene in Corbino Membrane Geometry. *ACS Nano* 4, 1889 (2010).
- [5] Berciaud, S. et al. Electron and Optical Phonon Temperatures in Electrically Biased Graphene. *Phys. Rev. Lett.* 104, 227401 (2010).
- [6] Bonini, N. Lazzeri, M. Marzari, N. Mauri, F. Phonon Anharmonicities in Graphite and Graphene. *Phys. Rev. Lett.* 99, 176802 (2007).
- [7] Song, D. et al. Direct Measurement of the Lifetime of Optical Phonons in Single-Walled Carbon Nanotubes. *Phys. Rev. Lett.* 100, 225503 (2008).
- [8] Jorio, A. G. et al. Joint density of electronic states for one isolated single-wall carbon nanotube studied by resonant Raman scattering. *Phys. Rev. B* 63, 245416 (2001).
- [9] Souza Filho, A. G. et al. Electronic transition energy  $E_{ii}$  for an isolated (n,m) single-wall carbon nanotube obtained by anti-Stokes/Stokes resonant Raman intensity ratio. *Phys. Rev. B* 63, 241404(R) (2001).
- [10] Klyshko, D. N. Correlation between the Stokes and anti-Stokes components in inelastic scattering of light. *Sov. J. Quantum Electron.* 7, 755 (1977).
- [11] Jorio, A. et al. Optical-Phonon Resonances with Saddle-Point Excitons in Twisted-Bilayer Graphene. *Nano Lett.* 14, 5687 (2014)
- [12] Lee, K. C. et al. Macroscopic non-classical states and terahertz quantum processing in room temperature diamond. *Nature Photon.* 6, 41 (2012).
- [13] Kasperczyk, M. Jorio, A. Neu, E. Maletinsky, P. and Novotny, L. Stokes-anti-Stokes Correlations in Raman Scattering from Diamond Membranes. <http://arxiv.org/abs/1503.00467>
- [14] Parra-Murillo, C. A. Santos, M. F. Monken, C. H. Jorio, A. Power dependence of Klyshko's Stokes-anti-Stokes correlation in the inelastic scattering of light. <http://arxiv.org/pdf/1503.01518v1.pdf>
- [15] Jorio, A. Cançado, L. G. Raman spectroscopy of twisted bilayer graphene. *Sol. Stat. Comm.* 175, 3 (2013).
- [16] Lui, C. H. Mak, K. F. Shan, J. Heinz T. F. Ultrafast Photoluminescence from Graphene. *Phys. Rev. Lett.* 105, 127404 (2010).
- [17] Herchen, H., Cappelli, M. A. First-order Raman spectrum of diamond at high temperatures. *Phys. Rev. B* 43, 11740 (1991).